

# Localization processes for functional data analysis

Antonio Elías<sup>1,2</sup>, Raúl Jiménez<sup>1,2</sup> and J. E. Yukich<sup>1,3\*</sup>

<sup>1</sup> Department of Statistics, Universidad Carlos III de Madrid

<sup>2</sup> UC3M-Santander Big Data Institute, Universidad Carlos III de Madrid

<sup>3</sup> Department of Mathematics, Lehigh University

October 28, 2021

## Abstract

We propose an alternative to  $k$ -nearest neighbors for functional data whereby the approximating neighbor curves are piecewise functions built from a functional sample. Instead of a distance on a function space we use a locally defined distance function that satisfies stabilization criteria. We exploit this feature to develop the asymptotic theory when the number of curves is large enough or when a finite number of curves is observed at time-points coinciding with the realization of a point process with intensity increasing to infinity. We use these results to investigate the problem of estimating unobserved segments of a partially observed functional data sample as well as to study the problem of functional classification and outlier detection. For these problems, we discuss methods that are competitive with and often superior to benchmark predictions in the field.

**Keywords**— Functional data; Nearest neighbors; Incomplete observations; Outlier detection.

---

\*Corresponding author. Email: joseph.yukich@lehigh.edu

# 1 Introduction

The  $k$ -nearest neighbors ( $k$ NN) method has been identified by IEEE as one of the top algorithms for solving multivariate statistical problems on large datasets (Wu et al., 2008). It is particularly useful for classification and regression, where the method is based on the idea that similar patterns must belong to the same class and near explanatory variables will have similar response variables. Among other applications of  $k$ NN in the multivariate setting, we can also include clustering (Brito et al., 1997), outlier detection (Ramaswamy et al., 2000) and time series forecasting (Martínez et al., 2017). Beyond its effectiveness, the popularity of the method is due in part to its conceptual ease and implementation. This has sparked the interest of researchers, who over many years have developed not only applications but also the mathematical theory, making the method an essential tool in nonparametric multivariate statistics. A critical review of the seminal literature on asymptotic theory related to the application of the method to classification, regression and density estimation is provided by Chapter 6 of Györfi et al. (2002).

In the context of functional data analysis (FDA), the  $k$ NN method has also been explored. For example, Zhang et al. (2010) address the problem of forecasting final prices of auctions via functional  $k$ NN and Hubert et al. (2017) construct classifiers for functional data also based on  $k$ NN. However, the asymptotic theory of these methods has remained undeveloped until now. Asymptotic results of methods based on functional  $k$ NN are mainly related to regression estimation when the response variable has finite dimension (Biau et al., 2010; Kudraszow and Vieu, 2013). Some of these results have been extended to other operations on the response variable (Kara et al., 2017), such as conditional distribution and conditional hazard function. And, exceptionally, Lian (2011) proves the consistency of some regression estimates based on  $k$ NN when both dependent and independent variables are functions. Thus, in the functional data setting, the mathematical theory of the  $k$ NN rule is unusually limited.

One of the purposes of this paper is to fill this lacuna and to provide the asymptotic theory for methods based on or inspired by  $k$ NN. The proofs of the main results rely on the theory of stabilizing functionals. This theory has been mainly developed for establishing limit theorems for statistics arising in stochastic geometry (Schreiber, 2010). At its core, this theory is applicable to statistics which are expressible as sums of score functions which depend on local data in a well-defined way. Statistics involving multivariate  $k$ NN are prime examples of locally defined score functions. In this context we study functional  $k$ NN. The key underlying idea is that the distance functions used in this paper are locally defined and satisfy stabilization criteria. This approach yields limits for the distances under consideration and shows that they converge to a distance function defined on a Poisson point process. While the intensity density of this Poisson point process depends on the observation time  $t$ , we show that the *expected* distance function does not. We exploit the fact that the distances are locally defined to rigorously develop their first and second order limit theory.

The second purpose of this paper is to review some problems of the FDA literature from

a perspective enriched by the new asymptotic results. In particular, we consider the problem of estimating unobserved values of a partially observed functional data sample, an important question prominently addressed in the literature (Kraus, 2015; Yao et al., 2005). As has been already reported (Zhang et al., 2010), the  $k$ NN method is a natural approach for addressing this problem. We show that the method may provide estimates that are superior to benchmark predictions in the field and we provide regularity conditions for guaranteeing their consistency. Also, we consider the problems of classification and outlier detection. Specifically, we introduce a probabilistic functional classifier inspired by the  $k$ NN rule. The classification method is based on the asymptotic normality of an empirical distance that only considers a finite number of sample curves but takes advantage of the infinite dimensionality of functional data. As far as we know, this type of asymptotic result is new and is particular to the functional setting. The problem of outlier detection is straightforwardly tackled by considering one-class classification. We carry out a comparative study with other widely used methods in FDA (Arribas-Gil and Romo, 2014; Li et al., 2012; Sun and Genton, 2011) that shows that our approach performs well across different test datasets. In addition, with the new classifier we may predict classification probabilities rather than only outputting the most likely class.

Functional data are typically viewed as independent realizations of a stochastic process with smooth trajectories observed on a compact interval (Yao et al., 2005). Consequently, we consider a stochastic process  $X = \{X(t) : t \in [a, b]\}$  with continuous sample paths. Following standard practice we set  $[a, b] = [0, 1]$ . Models for generating simulated functional data may imply that  $X(t)$  is unbounded for almost every  $t \in [0, 1]$ . This is the case of Fourier sums with Gaussian random coefficients, which frequently arise in simulation studies of functional data. However, the curves associated to many case studies are of bounded nature. Among some examples, we list mortality, fertility and migration rates (Hyndman and Ullah, 2007; Hyndman and Booth, 2008); curves of surface air temperatures and precipitation (Dai and Genton, 2018); electricity market data (Liebl, 2019) and functional data from many medical studies (Kraus, 2015; Yao et al., 2005). Either by definition, or for physical or biological restrictions, or for limitations of supply, functional data are often easily bounded. In line with this observation, we will assume for each  $t \in [0, 1]$  that  $X(t)$  belongs to a bounded interval. This assumption may differ from standard assumptions in the FDA literature but we believe that it correctly captures the properties of many real data. If we drop this assumption, then the asymptotic results presented here must be modified, including those concerning asymptotic expected values, variances, and distributions.

## 1.1 Definitions and terminology

Let  $X_1, \dots, X_n$  be independent copies of a stochastic process  $X$ . The classical way of defining a distance between sample paths  $X_i$  and  $X_j$  is to use the  $p$ -norm ( $p \geq 1$ ), also called Minkowski

distance,

$$D(X_i, X_j) = \left( \int_0^1 |X_i(t) - X_j(t)|^p dt \right)^{1/p}.$$

Other distances, such as the Hausdorff distance, can be defined from distances between two *nonaligned points* of the curves  $X_i$  and  $X_j$ . By two nonaligned points, we mean  $(t, X_i(t))$  and  $(s, X_j(s))$  with  $t \neq s$ . These type of distances are not considered in the present work. In any case, given a distance  $D(\cdot, \cdot)$  between two functions, the (global) nearest neighbor to  $X_i$  is defined by

$$X_i^{(1)} = \arg \min_{\{X_j: j \neq i\}} D(X_i, X_j).$$

Iterating, the global  $k$ NN to  $X_i$  is defined as the nearest neighbor in the subsample  $\{X_1, \dots, X_n\} \setminus \{X_i^{(1)}, \dots, X_i^{(k-1)}\}$ .

In this paper we also consider local nearest neighbors. We begin by considering the nearest sample piecewise function to  $X_i$ . This is the stochastic process

$$\hat{X}_i^{(1)}(t) = \arg \min_{\{X_j(t): j \neq i\}} |X_i(t) - X_j(t)|, \text{ for } t \in [0, 1]$$

which we call the *first localization process*. Thus this process consists of a union of sample curve segments which are the nearest sample observations to  $X_i$ . Now, we will define the  $k$ -nearest sample piecewise function to  $X_i$  by iterating, in way similar to how we defined  $X_i^{(k)}$ : First, for  $t \in [0, 1]$ , let  $G_i^0(t) = \{X_j(t) : j \neq i\}$ . Then, for  $1 \leq k \leq n$ , define  $G_i^k(t) = G_i^{k-1}(t) \setminus \{\hat{X}_i^{(k)}(t)\}$ . Thus, we define the  $k$ th localization process by

$$\hat{X}_i^{(k)}(t) = \arg \min_{x(t) \in G_i^{k-1}(t)} |X_i(t) - x(t)|. \quad (1)$$

The key statistics in this paper are the distances between the focal curve  $X_i$  and its  $k$ th localization process, called *localization distances* for short, and denoted by

$$L^{(k)}(X_i(t), \{X_j(t)\}_{j=1}^n) = |X_i(t) - \hat{X}_i^{(k)}(t)|, \quad t \in [0, 1].$$

The R package `localFDA` at <https://github.com/aefdzt/localFDA> provides the programs for computing the localization processes and localization distances.

Hereinafter, we assume that the marginal probability density of  $X(t)$ , denoted by  $\kappa_t$ , exists for almost all  $t \in [0, 1]$ . We have that  $\kappa_t$  integrates to one on its support, denoted by  $S(\kappa_t)$ , and assumed to be a finite union of bounded intervals. Let  $|A|$  denote the Lebesgue measure of the set  $A$ . The *re-scaled localization distance*

$$W_n^{(k)}(X_i(t), \{X_j(t)\}_{j=1}^n) = \frac{2n}{k|S(\kappa_t)|} \cdot L^{(k)}(X_i(t), \{X_j(t)\}_{j=1}^n), \quad (2)$$

that we use below, is the localization distance among the trajectories which have been properly scaled by  $2n/k|S(\kappa_t)|$ . This is

$$W_n^{(k)}(X_i(t), \{X_j(t)\}_{j=1}^n) = L^{(k)}\left(\frac{2n}{k|S(\kappa_t)|} X_i(t), \left\{ \frac{2n}{k|S(\kappa_t)|} X_j(t) \right\}_{j=1}^n\right).$$

We notice that the re-scaled localization distance  $W_n^{(k)}$  is invariant under any affine transformation of the data, i.e., transformations of the data by functions of the type  $T(x) = ax + b$  leave  $W_n^{(k)}$  unchanged. Both the results and methods discussed in this paper are invariant under affine transformations.

## 1.2 Outline of this work

This paper is organized as follows. Section 2 presents three types of asymptotic results.

- (a) Weak laws for  $W_n^{(k)}(X_i(t), \{X_j(t)\}_{j=1}^n)$ , at a fixed  $t \in [0, 1]$ , when  $n$  goes to infinity.
- (b) Asymptotic normality as  $n \rightarrow \infty$  for  $\sum_{i \in I_n} W_n^{(k)}(X_i(t), \{X_j(t), j \in J_n\})$ ,  $t \in [0, 1]$  fixed, when  $I_n$  and  $J_n$  are index sets whose cardinality increases up to infinity as  $n \rightarrow \infty$ .
- (c) Asymptotic normality for  $\sum_{t \in \mathcal{T}} L^{(k)}(X_i(t), \{X_j(t)\}_{j=1}^n)$ , for a fixed number of curves  $n$ , when  $\mathcal{T}$  is a set of random locations whose cardinality increases up to infinity.

Limit theorems of type (a) and (b) are used in Section 3, where we consider estimation of missing values on partially observed data via  $k$ NN. Limit theorems of type (c) are used in Section 4, which provides a new method for classification and outlier detection. A general discussion of both theoretical and practical results is presented in Section 5 whereas Section 6 provides the proofs of our claims presented in Section 2.

## 2 Asymptotic results

### 2.1 Weak laws for re-scaled distances with large data sizes

**Theorem 2.1.** *For all integers  $k \in \mathbb{N}$  and almost all  $t \in [0, 1]$ , we have*

$$\lim_{n \rightarrow \infty} \mathbb{E} W_n^{(k)}(X_1(t), \{X_j(t)\}_{j=1}^n) = 1 \quad (3)$$

and if  $\kappa_t$  is bounded away from zero on its support  $S(\kappa_t)$  then

$$\lim_{n \rightarrow \infty} \text{Var}[W_n^{(k)}(X_1(t), \{X_j(t)\}_{j=1}^n)] = \left(1 + \frac{1}{k}\right) \int_{S(\kappa_t)} \frac{1}{\kappa_t(y)} dy - 1. \quad (4)$$

In addition, as  $n \rightarrow \infty$ ,

$$W_n^{(k)}(X_1(t), \{X_j(t)\}_{j=1}^n) \xrightarrow{\mathcal{D}} \frac{2}{k|S(\kappa_t)|} \cdot L^{(k)}(\mathbf{0}, \mathcal{P}_{\kappa_t}(X_1(t))), \quad (5)$$

$\mathcal{P}_{\kappa_t}(X_1(t))$  being the Cox point process given by the Poisson point process on  $\mathbb{R}$  with a variable intensity density  $\kappa_t(X_1(t))$ .

The limit (3) says the expectation of the re-scaled distance converges to one for all values of  $k$  and almost all values of  $t$  and  $\kappa_t$ . Thus, the asymptotic expected error in locating a

typical curve by its  $k$ th localization process is roughly  $k|S(\kappa_t)|/2n$ , which depends on  $k$  and on the Lebesgue measure of the support of the underlying distribution of the data at the time of observation. As a by-product of the proof of (5), we find an asymptotic formula for the expected re-scaled distance at a given height  $y \in [0, 1]$ . Small distances correspond to highly concentrated data, as expected. We find that if  $\kappa_t$  is bounded away from zero, then for all  $k \in \mathbb{N}$  and almost all  $t \in [0, 1]$

$$\lim_{n \rightarrow \infty} \mathbb{E} W_n^{(k)}(X_1(t), \{X_j(t)\}_{j=1}^n | X_1(t) = y) = \frac{1}{\kappa_t(y)}.$$

We next consider the case when  $k := k(n)$  increases with  $n$  and there are a Poisson number  $N(n)$  of curves, where  $N(n)$  is a Poisson random variable with mean  $n$ .

**Theorem 2.2.** *Let  $\kappa_t$  be  $\alpha$ -Hölder continuous, i.e., there is  $\alpha \in (0, 1]$  such that*

$$|\kappa_t(x) - \kappa_t(y)| \leq C|x - y|^\alpha, \quad x, y \in S(\kappa_t).$$

*Let  $k := k(n)$  satisfy  $\lim_{n \rightarrow \infty} k^{1+\alpha}/n^\alpha = 0$ . Then*

$$\lim_{n \rightarrow \infty} \mathbb{E} W_n^{(k)}(X_1(t), \{X_j(t)\}_{j=1}^{N(n)}) = 1 \quad (6)$$

*and if  $\kappa_t$  is bounded away from zero on its support  $S(\kappa_t)$  then*

$$\lim_{n \rightarrow \infty} \text{Var}[W_n^{(k)}(X_1(t), \{X_j(t)\}_{j=1}^{N(n)})] = \int_{S(\kappa_t)} \frac{1}{\kappa_t(y)} dy - 1. \quad (7)$$

The right hand side of (7) is zero if  $\kappa_t$  is uniform on its support. So, in this particular case, we have  $W_n^{(k)}(X_1(t), \{X_j(t)\}_{j=1}^{N(n)})$  converges to one in probability.

## 2.2 Asymptotic normality of average distances for large $n$

When functional data are partially observed, some sample functions are observed at time  $t$  whereas others are not (Kneip and Liebl, 2020; Kraus, 2015; Yao et al., 2005). For modeling this setting, we suppose we have a total of  $N(n)$  curves,  $N(n)$  being a Poisson random variable with mean  $n$ , and a proportion of them, say  $pN(n)$ , are not observed at  $t$ . Therefore, only  $(1 - p)N(n)$  are available for computing the localization process at  $t$ .

Formally, for each  $t \in [0, 1]$ , we let  $X_i(t), 1 \leq i \leq N(n)$ , be a marked point process with values in  $\mathbb{R} \times \mathbb{M}$ , where the mark space  $\mathbb{M} := \{0, 1\}$  is equipped with a measure  $\mu_{\mathbb{M}}$  giving probability  $p$  to  $\{1\}$  and probability  $1 - p$  to  $\{0\}$ . If the mark at  $X_i(t)$  equals one, then it comes from a curve whose value is unknown at time  $t$ , whereas if a mark at a point equals zero, then it comes from the collection of curves whose values are known at time  $t$  and which are thus used to construct the localization process at  $t$ . In general, the marks for  $X_i(t_1)$  and  $X_i(t_2)$  are different for  $t_1 \neq t_2$ . We write  $\tilde{X}_i(t)$  to denote the point  $X_i(t)$  equipped with a mark. Let

$I_m(t), m \in \{0, 1\}$ , be the set of indices  $i$ 's for which  $\tilde{X}_i(t)$  has mark equal to  $m$ . This gives the statistic

$$W_n^{(k)}\left(\tilde{X}_i(t), \{\tilde{X}_j(t)\}_{j=1}^{N(n)}\right) = W_n^{(k)}(X_i(t), \{X_j(t), j \in I_0(t)\})$$

defined as the re-scaled distance (2) but only based on the available (observed) points at  $t$ .

To develop the second order limit theory, we write  $\tilde{x}$  to denote the point  $x$  equipped with a mark. We write  $\tilde{\mathcal{P}}_{\kappa_t(y)}$  for the Poisson point process  $\mathcal{P}_{\kappa_t(y)}$  where each point is equipped with an independent mark having measure  $\mu_{\mathbb{M}}$ , and we put

$$\begin{aligned} \tilde{\sigma}_t^2 := & \int_{S(\kappa_t)} \mathbb{E}(L^{(k)}(\tilde{\mathbf{0}}, \tilde{\mathcal{P}}_{\kappa_t(y)}))^2 \kappa_t(y) dy \\ & + \int_{S(\kappa_t)} \int_{\tilde{x} \in \tilde{\mathbb{R}}} [\mathbb{E}(L^{(k)}(\tilde{\mathbf{0}}, \tilde{\mathcal{P}}_{\kappa_t(y)} \cup \{\tilde{x}\}) L^{(k)}(\tilde{x}, \tilde{\mathcal{P}}_{\kappa_t(y)} \cup \{\tilde{\mathbf{0}}\}) \\ & - \mathbb{E}(L^{(k)}(\tilde{\mathbf{0}}, \tilde{\mathcal{P}}_{\kappa_t(y)}) \mathbb{E} L^{(k)}(\tilde{x}, \tilde{\mathcal{P}}_{\kappa_t(y)})](\kappa_t(y))^2 d\tilde{x} dy. \end{aligned} \quad (8)$$

Let  $d_K(X, Y)$  be the Kolmogorov distance between random variables  $X$  and  $Y$  and let  $N(\mu, \sigma^2)$  denote a normal random variable centered at  $\mu$  with variance equal to  $\sigma^2$ .

**Theorem 2.3.** *We assume that  $\kappa_t$  is Lipschitz and bounded away from zero on its support  $S(\kappa_t)$ . We have for  $p \in [0, 1)$  and  $k \in \mathbb{N}$*

$$\frac{\sum_{i \in I_0(t)} \left( W_n^{(k)}\left(\tilde{X}_i(t), \{\tilde{X}_j(t)\}_{j=1}^{N(n)}\right) - (1-p)^{-1} \right)}{\sqrt{n(1-p)}} \xrightarrow{\mathcal{D}} N\left(0, \nu^2(t, k)\right) \quad (9)$$

where

$$\nu^2(t, k) = \lim_{n \rightarrow \infty} \frac{\text{Var} \sum_{i \in I_0(t)} W_n^{(k)}\left(\tilde{X}_i(t), \{\tilde{X}_j(t)\}_{j=1}^{N(n)}\right)}{n(1-p)} = \frac{4\tilde{\sigma}_t^2}{(1-p)^2 k^2} \quad (10)$$

and where  $\tilde{\sigma}_t^2$  is at (8). Moreover for all  $k \in \mathbb{N}$  there is a constant  $C_1(k)$  such that

$$d_K \left( \frac{\sum_{i \in I_0(t)} \left( W_n^{(k)}\left(\tilde{X}_i(t), \{\tilde{X}_j(t)\}_{j=1}^{N(n)}\right) - (1-p)^{-1} \right)}{\sqrt{\text{Var} \sum_{i \in I_0(t)} W_n^{(k)}\left(\tilde{X}_i(t), \{\tilde{X}_j(t)\}_{j=1}^{N(n)}\right)}}, N(0, 1) \right) \leq \frac{C_1(k)}{\sqrt{n}}. \quad (11)$$

Also we have for  $p \in (0, 1)$

$$d_K \left( \frac{\sum_{i \in I_1(t)} \left( W_n^{(k)}\left(\tilde{X}_i(t), \{\tilde{X}_j(t)\}_{j=1}^{N(n)}\right) - (1-p)^{-1} \right)}{\sqrt{\text{Var} \sum_{i \in I_1(t)} W_n^{(k)}\left(\tilde{X}_i(t), \{\tilde{X}_j(t)\}_{j=1}^{N(n)}\right)}}, N(0, 1) \right) \leq \frac{C_1(k)}{\sqrt{n}} \quad (12)$$

and

$$\lim_{n \rightarrow \infty} \frac{\text{Var} \sum_{i \in I_1(t)} W_n^{(k)}\left(\tilde{X}_i(t), \{\tilde{X}_j(t)\}_{j=1}^{N(n)}\right)}{\text{Var} \sum_{i \in I_0(t)} W_n^{(k)}\left(\tilde{X}_i(t), \{\tilde{X}_j(t)\}_{j=1}^{N(n)}\right)} = \frac{p}{1-p}. \quad (13)$$

Theorem 2.3 provides asymptotic confidence intervals for the average error when replacing unobserved curves with their corresponding localization processes. This average error is

$$\begin{aligned}\bar{L}^{(k)}(t) &:= \frac{1}{\text{card}[I_1(t)]} \sum_{i \in I_1(t)} L_n^{(k)}\left(\tilde{X}_i(t), \{\tilde{X}_j(t)\}_{j=1}^{N(n)}\right) \\ &= \frac{1}{\text{card}[I_1(t)]} \frac{k|S(\kappa_t)|}{2n} \sum_{i \in I_1(t)} W_n^{(k)}\left(\tilde{X}_i(t), \{\tilde{X}_j(t)\}_{j=1}^{N(n)}\right),\end{aligned}\tag{14}$$

with  $\text{card}[A]$  being the cardinality of  $A$ . In fact, Theorem 2.3 and Slutsky's theorem imply that, if  $n$  is large enough, the distribution of  $\bar{L}^{(k)}(t)$  is approximately normal with mean equal to  $(k|S(\kappa_t)|/2n) \cdot 1/(1-p)$  and variance equal to  $(k|S(\kappa_t)|/2n)^2 \cdot \nu^2(t, k)/np$ . We observe that these values are, respectively,  $O(k/n)$  and  $O(k^2/n^3)$ . To verify the latter, we require that  $\tilde{\sigma}_t^2$  at (8) increases as  $k^2$ . This can be seen from the proof of (4).

Leaving aside the statistical applications that involve partially observed functional data, we remark that Theorem 2.3 also establishes a central limit theorem for the sum of the localization distances when all the curves are completely observed. This corresponds to the case  $p = 0$ . It shows, given a Poisson point process on the interval  $[0, 1]$  with intensity density  $n\kappa_t$ , that the sum of the re-scaled distances between points of this point process and their  $k$ th nearest neighbors is asymptotically normal as  $n \rightarrow \infty$ . The case  $p = 0$  is a special case of a more general result of Penrose and Yukich (2001) giving the total edge length of the  $k$  nearest neighbors graph on Poisson input in all dimensions when the entirety of the input is used.

## 2.3 Stochastic behavior of empirical localization distances

We often observe the functional data on a discrete grid  $\{t_1, \dots, t_m\}$ . In such cases, we are interested in the average distance between  $X_i$  and its  $k$ th localization process (1) as a global measure of nearness. This is

$$L_i^{(k)} = \frac{1}{m} \sum_{r=1}^m L^{(k)}(X_i(t_r), \{X_j(t_r)\}_{j=1}^n).\tag{15}$$

Here we focus on the random behavior of  $L_i^{(k)}$  when the localization distances are evaluated at the locations of a point process. This gives rise to the notion of an empirical localization process and goes as follows. Let  $t_1, t_2, \dots, t_M$  be the realization of a homogeneous Poisson point process  $\mathcal{P}_\lambda$  in  $[0, 1]$  having intensity  $\lambda \in (0, \infty)$ . Here  $M := M(\lambda)$  is a Poisson random variable with parameter  $\lambda$ . We fix  $n$ , the number of data curves. We then evaluate the localization distance with respect to  $X_i$  at each  $t_r$  in  $\mathcal{P}_\lambda$ . This generates the so-called *empirical localization distance* between  $X_i$  and its  $k$ th localization process namely

$$\frac{1}{M} \sum_{r=1}^M L^{(k)}(X_i(t_r), \{X_j(t_r)\}_{j=1}^n).\tag{16}$$



The empirical localization distance is simply the localization distance  $L_i^{(k)}$  averaged over the points of  $\mathcal{P}_\lambda$ . In particular, for all  $\lambda$  fixed, the Mecke formula and Theorem 2.1 give as  $n \rightarrow \infty$

$$\mathbb{E} \frac{1}{M} \sum_{t_r \in \mathcal{P}_\lambda} W_n^{(k)}(X_i(t_r), \{X_j(t_r)\}_{j=1}^n) \rightarrow 1.$$

The localization distances  $L(t) := L^{(k)}(X_i(t), \{X_j(t)\}_{j=1}^n)$ ,  $t \in \mathcal{P}_\lambda$ , in general exhibit dependence. However, if  $L(t')$ ,  $t' \in \mathcal{P}_\lambda$ , depends only on the values of  $L(\cdot)$  at ‘nearby’ data points  $t \in \mathcal{P}_\lambda$ , then we may establish the asymptotic normality of sums of localization distances, as in the next result. Here, by ‘nearby’ we mean the points  $t$  in  $\mathcal{P}_\lambda$  which are neighbors to  $t'$ .

In contrast to Theorem 2.3, the next theorem focusses on the behavior of the average localization distances around a particular curve as the number of sampling observations increases to infinity. This theorem follows from general central limit theorems for local dependence structures allowing one to use dependency graph arguments, as explained in Theorem 2.2 of Rinott and Rotar (1996). The localization distances are bounded by 1 and thus satisfy moment bounds of all order. The following theorem consequently follows from standard arguments of Penrose and Yukich (2005) and hence we will omit its proof.

**Theorem 2.4.** *Fix  $n$ , the number of data functions. We consider the distance between  $X_i$  and its  $k$ th localization process, namely  $L(t) := L^{(k)}(X_i(t), \{X_j(t)\}_{j=1}^n)$ . Let  $\mathcal{P}_\lambda$  be a homogeneous Poisson point process with intensity  $\lambda$  on  $[0, 1]$ . Assume that the random variables  $L(t)$ ,  $t \in \mathcal{P}_\lambda$ , exhibit  $l$  nearest neighbor dependencies, namely, the value of  $L(t)$ ,  $t \in \mathcal{P}_\lambda$ , depends only on the values of  $L(t_1), \dots, L(t_l)$ , where  $t_1, \dots, t_l$  are the  $l$  nearest neighbors to  $t$  in the Poisson sample  $\mathcal{P}_\lambda$ . Then as  $\lambda \rightarrow \infty$  we have*

$$\frac{\sum_{t \in \mathcal{P}_\lambda} (L(t) - \mathbb{E}L(t))}{\sqrt{\text{Var}[\sum_{t \in \mathcal{P}_\lambda} L(t)]}} \xrightarrow{\mathcal{D}} N(0, 1). \quad (17)$$

The expected value and the variance in (17) can be estimated by the sample mean and sample variance of the average localization distances induced by the points of  $\mathcal{P}_\lambda$ . These are

$$\bar{L}^{(k)} = \frac{1}{n} \sum_{i=1}^n L_i^{(k)} \quad \text{and} \quad S_L^2 = \frac{1}{n-1} \sum_{i=1}^n (L_i^{(k)} - \bar{L}^{(k)})^2.$$

Thus, when  $n$  is large, the score at the left hand side of (17) is roughly  $T_i^{(k)} = (L_i^{(k)} - \bar{L}^{(k)})/S_L$ . Theorem 2.4 suggests that the statistics  $T_i^{(k)}$  could be used for testing whether  $X_i$  is properly localized by the data in accordance with an underlying Gaussian distribution. We explore this idea for classification and outlier detection in Section 4.

### 3 Reconstruction of partially observed data via $k$ NN

One might hope that two smooth curves that are near on a set  $S \subset [0, 1]$  and which are copies of the same process should remain near on  $[0, 1] \setminus S$ . In particular, if  $S$  is blindly chosen and with large Lebesgue measure, one could hope to achieve this proximity without taking into account any prior morphological information, such as shape and complexity, of the sample curves. Here we show that this turns out to be the case, subject to mild assumptions on the data. This is achieved by making use of  $k$ -nearest neighbor methods for reconstructing partially observed data.

As is customary in the literature, we model partially observed functional data by considering a random mechanism  $Q$  that generates compact subsets of  $[0, 1]$ . These sets correspond to ranges where sample paths are observed. Formally,  $O_1, \dots, O_n$  are independent random closed sets from  $Q$  such that  $X_i$  is observed on  $O_i$  and is missed on  $M_i = [0, 1] \setminus O_i$ . We also will assume data are Missing-Completely-At-Random, i.e. the sets  $\{O_i\}$  are independent of the sample paths (Kneip and Liebl, 2020). Without loss of generality, suppose also that there is no time which is almost surely censored. That is to say we assume  $\mathbb{P}(O_i \text{ contains } s) > 0$  for almost all  $s \in [0, 1]$ .

To simplify the notation, consider first the case in which just one sample path is partially observed, say  $X_1$ . Therefore we assume for now that  $X_2, \dots, X_n$  are fully observed on  $[0, 1]$ . Instead of Minkowski distances taken on the complete observation range  $[0, 1]$ , we now consider the distances to  $X_1$  restricted to  $O_1$ , namely

$$D_p(X_j) = \left( \int_{O_1} |X_j(t) - X_1(t)|^p dt \right)^{1/p}. \quad (18)$$

Denote by  $X^{(j)}$  the  $j$ NN to  $X_1$  with respect to this distance. In order to estimate  $X_1$  on  $M_1$ , we adopt the  $k$ NN methodology and consider convex combinations of the form  $\sum_{j=1}^r w_j \cdot X^{(j)}$ . The choice of  $r$  and suitable weights  $\{w_j\}_{j=1}^r$  will be discussed later. We start by providing conditions for the consistency of this type of estimator. For this, it is enough to discuss conditions for the consistency of  $X^{(j)}$  as an estimator of  $X_1$ .

Choose an arbitrary  $l \neq 1$  and consider the random set on which the  $X_l$  is closer than the  $k$ th localization process  $\hat{X}_1^{(k)}$ . That is to say we consider the set

$$I^{(k)}(X_l) = \left\{ t \in [0, 1] : |X_l(t) - X_1(t)| \leq |\hat{X}_1^{(k)}(t) - X_1(t)| \right\}. \quad (19)$$

Note  $\mathbb{P}(I^{(k)}(X_l) \text{ contains } s) = k/(n-1)$  for all  $s \in [0, 1]$ . Since  $X^{(j)}$  is selected by its proximity to  $X_1$  on  $O_1$ , and since  $O_1$  is independent of  $X_1$  and  $\hat{X}_1^{(k)}$ , one expects, as  $k$  increases up to  $n$ , that  $\mathbb{P}(I^{(k)}(X^{(j)}) \text{ contains } s)$  increases up to 1 faster than  $\mathbb{P}(I^{(k)}(X_l) \text{ contains } s)$  for any fixed  $j$  and  $s \in [0, 1]$ . More formally, we will consider the following assumption:

$$\lim_{n \rightarrow \infty} \mathbb{P}(I^{(k)}(X^{(j)}) \text{ contains } s) \rightarrow 1 \text{ for some } k = o(\sqrt{n}), \quad s \in [0, 1]. \quad (20)$$

Given the features of many functional data used in practice, condition (20) does not appear too unusual. In many cases, the functions are smoothed data coming from truncated Fourier series. This is the reason why simulation studies often consider Fourier sums with random coefficients for generating test data. In this context we note that Fourier sums are close to a target curve whenever the respective coefficients are close. Moreover, if the Fourier sums are close to a target on an observable window in  $[0, 1]$ , then they are close everywhere in  $[0, 1]$ , since the coefficients do not depend on  $t$ . In such cases, if  $j$  is fixed one expects the  $j$ NN to be roughly at a distance  $O(1/n)$ . On the other hand, if  $k = o(\sqrt{n})$ , the  $k$ th localization process is at a distance  $o(1/\sqrt{n})$ , verifying (20). As an illustration, Figure 1 shows empirical estimators of  $\mathbb{P}(I^{(k)}(X^{(j)}) \text{ contains } s)$  based on 1000 replicates of  $(X_1, O_1)$ , when  $n = 2500$  and  $k$  up to 250.  $O_1$  is obtained by removing at random one of the three closed intervals of the subdivision of  $[0, 1]$  induced by two independent  $\text{Uniform}(0,1)$  random variables.  $X_i$  is a linear combination of sines and cosines with independent normal coefficients, as those used for generating data in previous studies (Kneip and Liebl, 2020; Kraus, 2015).

**Proposition 1.** *Suppose  $\kappa_t$  is Lipschitz continuous and that (20) holds. Then for any fixed  $j$  and all  $\varepsilon > 0$  we have*

$$\lim_{n \rightarrow \infty} \mathbb{P}(|X^{(j)}(t) - X_1(t)| < \varepsilon) = 1.$$

*Proof.* Denote  $A(t, \varepsilon) = \{|X^{(j)}(t) - X_1(t)| > \varepsilon\}$ . We have

$$\begin{aligned} \mathbb{P}(A(t, \varepsilon)) &= \mathbb{P}(A(t, \varepsilon); t \in I^{(k)}(X^{(j)})) + \mathbb{P}(A(t, \varepsilon); t \notin I^{(k)}(X^{(j)})) \\ &\leq \frac{1}{\varepsilon} \mathbb{E}[|X^{(j)}(t) - X_1(t)|; t \in I^{(k)}(X^{(j)})] + \mathbb{P}(t \notin I^{(k)}(X^{(j)})) \\ &\leq \frac{1}{\varepsilon} \mathbb{E}[|X_1^{(k)}(t) - X_1(t)|; t \in I^{(k)}(X^{(j)})] + \mathbb{P}(t \notin I^{(k)}(X^{(j)})) \\ &\leq \frac{1}{\varepsilon} \mathbb{E}[|X_1^{(k)}(t) - X_1(t)|] + \mathbb{P}(t \notin I^{(k)}(X^{(j)})) \\ &\leq \frac{k|S(\kappa_t)|}{2n\varepsilon} \mathbb{E}[W_n^{(k)}(X_1(t), \{X_j(t)\}_{j=1}^n)] + \mathbb{P}(t \notin I^{(k)}(X^{(j)})). \end{aligned}$$

Since  $\kappa_t$  is Lipschitz, we can apply Theorem 2.2 for  $\alpha = 1$  and  $k := k(n) = o(\sqrt{n})$ . Thus, as  $n \rightarrow \infty$ , the right hand side goes to 0 by Theorem 2.2 and (20).  $\square$

As is customary, we suppose there is a proportion of curves completely observed. In that case, we can repeat the above approach for estimating any sample curve partially observed by choosing its  $j$ NN from among the curves which are fully observed. Moreover, as we remarked, if there is a significantly large proportion of curves with missed values at  $t$ , then Theorem 2.3 provides asymptotic confidence intervals for average errors when imputing missing values by localization processes. In view of our construction, if  $k$  is large but finite, these errors can be used for bounding, with significantly high probability, errors resulting when estimating missing values by nearest neighbors. In other words, if (19) holds, based on Theorem 2.3 we are able to provide approximate confidence intervals for average errors when estimating by nearest

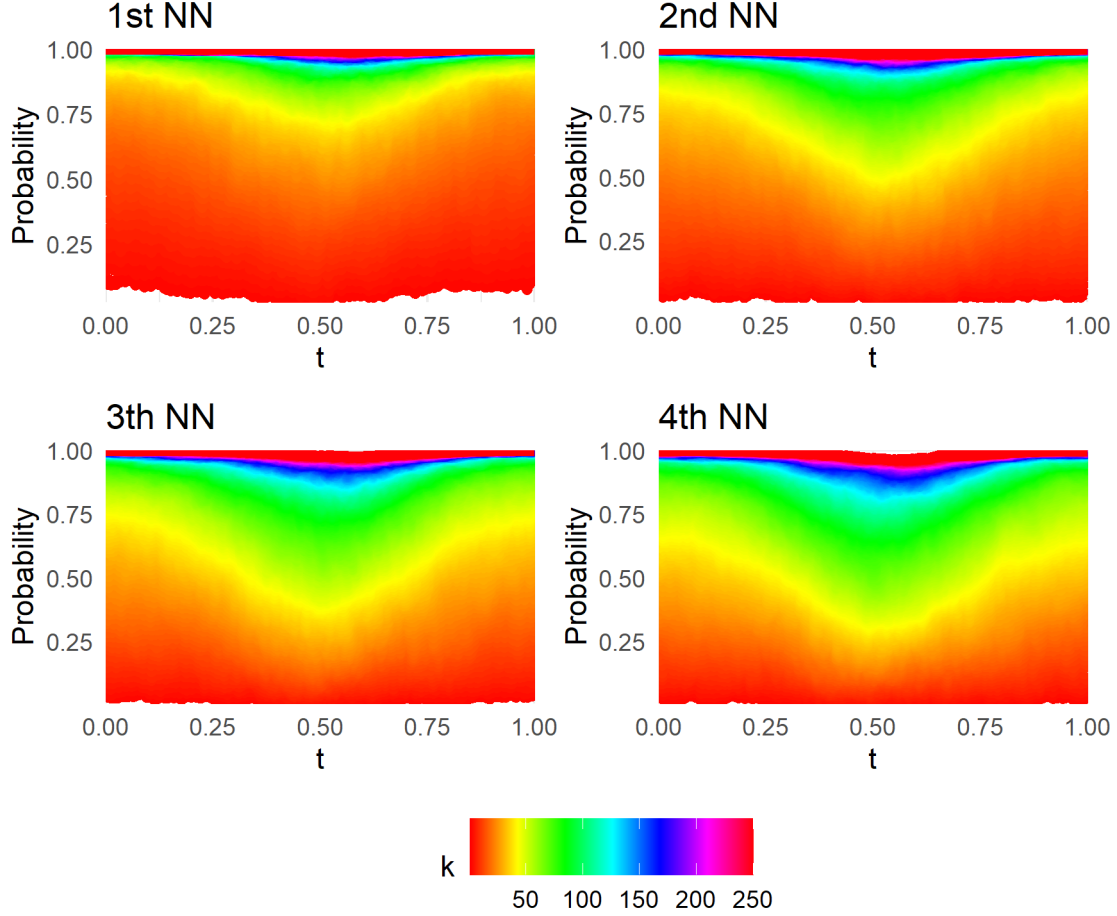


Figure 1: Estimated values of  $\mathbb{P}(I^{(k)}(X^{(j)}) \text{ contains } t)$ ,  $0 \leq t \leq 1$ ,  $1 \leq j \leq 4$ ,  $1 \leq k \leq 250$ ,  $n = 2500$ . The estimation is based on 1000 independent replicates of  $(X_1, O_1)$  when  $O_1$  is obtained by removing randomly one interval of the partition of  $[0, 1]$  induced by two independent  $\text{Uniform}(0, 1)$  variables.  $X_i$  is a linear combination of sines and cosines with independent Gaussian coefficients.

neighbors. In particular, following the discussion around (14), these average errors are  $O(k/n)$  in mean, with variance  $O(k^2/n^3)$ . This is an additional attraction of the  $k$ NN estimators that we describe in detail below.

Let us go back to the simplest case, where the curve  $X_1$  is observed on  $O_1$  and unobserved on  $M_1$ , where  $X_2 \dots, X_n$  are fully observed on all the observation range, and where the  $k$ NN estimator of  $X_1(t)$  has the form

$$\hat{X}_{k\text{NN}} = \sum_{j=1}^r w_j \cdot X^{(j)}(t),$$

with  $w_j > 0$ , for  $1 \leq j \leq k$ , and  $\sum_{j=1}^r w_j = 1$ . We follow previous literature (Hubert et al.,

2017; Zhang et al., 2010) and consider Minkowski distances with  $p = 1$  and  $p = 2$ . In the forecasting context, both functional data and univariate time series, the weights for these Minkowski distances have been already suggested (Zhang et al., 2010; Martínez et al., 2017). We use these recommendations and set  $w_j = D_p(X^{(j)})^{-p} / \sum_{i=1}^r D_p(X^{(i)})^{-p}$ ,  $D_p(\cdot)$  being the distance to  $X_1$  defined in (18). The value of  $r$  used to define the  $k$ NN estimator is chosen by minimizing the mean square error between the estimator and the target function  $X_1$  on the observation range. This is

$$r = \arg \min_r \int_{O_1} |\hat{X}_{k\text{NN}}(t) - X_1(t)|^2 dt.$$

The Mean Square Errors on  $M_1$  (MSE), that is to say  $\int_{M_1} |\hat{X}(t) - X_1(t)|^2 dt$ , are used for evaluating the estimator performance.

To illustrate the method, we conducted a simulation study based on two real case studies. The differences between the results obtained by the functional  $k$ NN method based on the Minkowski distance with  $p = 1$  and  $p = 2$  were negligible, being slightly superior for  $p = 2$ . Hence, in order to summarize information, we only report results for  $p = 2$ .

### 3.1 Yearly curves of Spanish temperatures

Yearly curves of daily temperatures are common in FDA (Dai and Genton, 2018; López-Pintado and Romo, 2009; Ramsay and Silverman, 2005). We consider 2786 such curves from 73 weather stations located in capital cities of 50 Spanish regions (provinces). The data was obtained from <http://www.aemet.es/>, the Meteorological State Agency of Spain (AEMET) website. The date at which the data was first recorded varies from station to station. For example, the Madrid-Retiro station reports records from 1893 onwards whereas the Barcelona-Airport started in 1925 and Ceuta from 2003. On the other hand, it is likely that some states failed at some moment to record data. The point is that there are several incomplete years (Febrero-Bande et al., 2019). With the aim to estimate the missing data, we test several methods with a simulation study based on this data set. From the 2786 fully observed curves we selected one at random, labeled as  $X_1$ , at which we censored a random number of consecutive days. Term  $O_1$  represents the uncensored days. The average number of censored days was 122, a third of the year. We repeat this procedure 1000 times and estimate the censored data by using  $k$ NN and the following benchmark methods that we name by acronyms to refer to them in what follows:

1. KL20 (Kneip and Liebl, 2020). This is novel reconstruction method belongs to a new class of functional operators. The used code was obtained from a repository by the authors (<https://github.com/lidom/ReconstPoFD>).
2. KRAUS (Kraus, 2015). This is one of the more powerful methodologies for completing functional data based on principal component analysis. The code was obtained from the

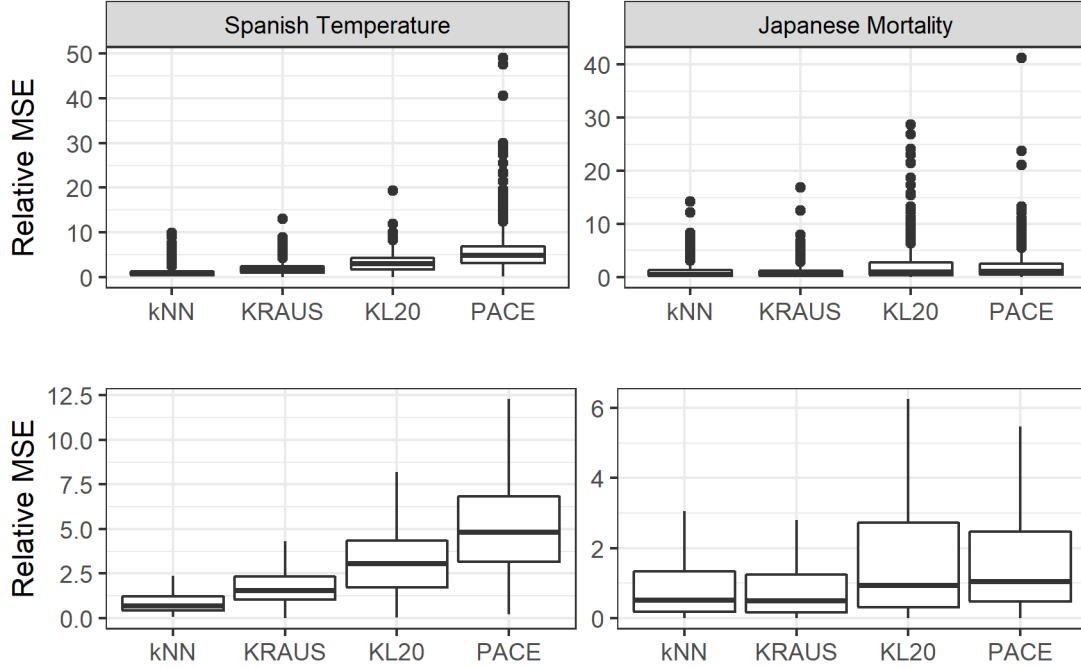


Figure 2: Top panels: Boxplots of Relative MSE from 1000 reconstruction exercises based on yearly curves of Spanish daily temperatures and Japanese mortality rates. Bottom panels: Zooms around the median of the above boxplots by excluding atypical values.

authors website ([https://is.muni.cz/www/david.kraus/web\\_files/papers/partial\\_fda\\_code.zip](https://is.muni.cz/www/david.kraus/web_files/papers/partial_fda_code.zip)).

3. PACE (Yao et al., 2005). This is the most cited nonparametric method when performing principal component analysis on sparse longitudinal data. For implementation, we used the code from the package `fdapace` (Chen et al., 2020).

By far the best method was  $k$ NN. For ease in interpreting the results, we report *Relative* MSE, namely the MSE divided by the MSE average when applying the  $k$ NN method. This shows that the MSE associated with  $k$ NN are roughly one half the MSE for KRAUS, a third of MSE for  $KL20$  and a fifth of PACE MSE. This can be observed from the boxplots of Relative MSE on the left side of Figure 2). On the bottom of this figure, we zoom in on these boxplots around the median by excluding the atypical values. In addition, although all the methods are computationally efficient,  $k$ NN resulted in being the most efficient (see Table 1).

Figure 3 (Left panels) illustrates the typical performance of each method. Although all the methods estimate correctly the mean temperature over the daily range, their estimated curve may be somewhat flattened, without the typical oscillations of Spanish daily temperatures.

	kNN	KRAUS	KL20	PACE
Spanish Temperature	<b>0.1351</b> ( <b>0.1134</b> )	7.4478 (1.7490)	3.4935 (10.487)	4.0523 (0.3510)
Japanese Mortality	<b>0.0197</b> ( <b>0.0164</b> )	0.0980 (0.0554)	2.5640 (1.1701)	6.6073 (3.4661)

Table 1: Mean running time in seconds observed from 1000 reconstruction exercises based on yearly curves of Spanish daily temperatures and Japanes age-specific mortality rates. Standard deviations are between parentheses.

Only the  $k$ NN method provide estimators that may catch both the values of the curve and its shape.

An additional attractive of  $k$ NN is its easy interpretation. The right panels of Figure 3 show the  $k$ NN of the curve under reconstruction, allowing one to observe that the curves used for estimating come from stations sharing similar weather and which was recorded in similar years.

### 3.2 Japanese age-specific mortality rates

The Human Mortality Data Set (University of California, Berkeley (USA) and Max Planck Institute for Demographic Research (Germany), 2019) provides detailed mortality and population data of 41 countries or areas. For some countries, they also offer micro information by subdivision of the territory, providing data which is rich in spatio-temporal information. A FDA approach to analyze mortality data is to consider age-specific mortality rates as sample functions (Gao et al., 2019; Shang and Hyndman, 2017). In particular, the Japanese mortality dataset is available for its 47 prefectures in many years. However, the curves of some prefectures are incomplete during some years. In total, we obtained 2007 complete curves of Japanese age-specific mortality rates with data between 1975 and 2016. We used these curves for comparing the reconstruction methods under consideration by repeating the simulation setup described in the previous subsection. All the methods perform well on these data. Typically they do not have the strong oscillations exhibited by the Spanish temperatures (see the supplementary material for some illustrations). KRAUS performed better than  $k$ NN, although the difference was negligible. Both methods worked better than PACE and KL20. These results are summarized on boxplots of MSE in Figure 2, as done already with the simulations based on Spanish temperatures. The computational efficiency of  $k$ NN is reported in Table 1.

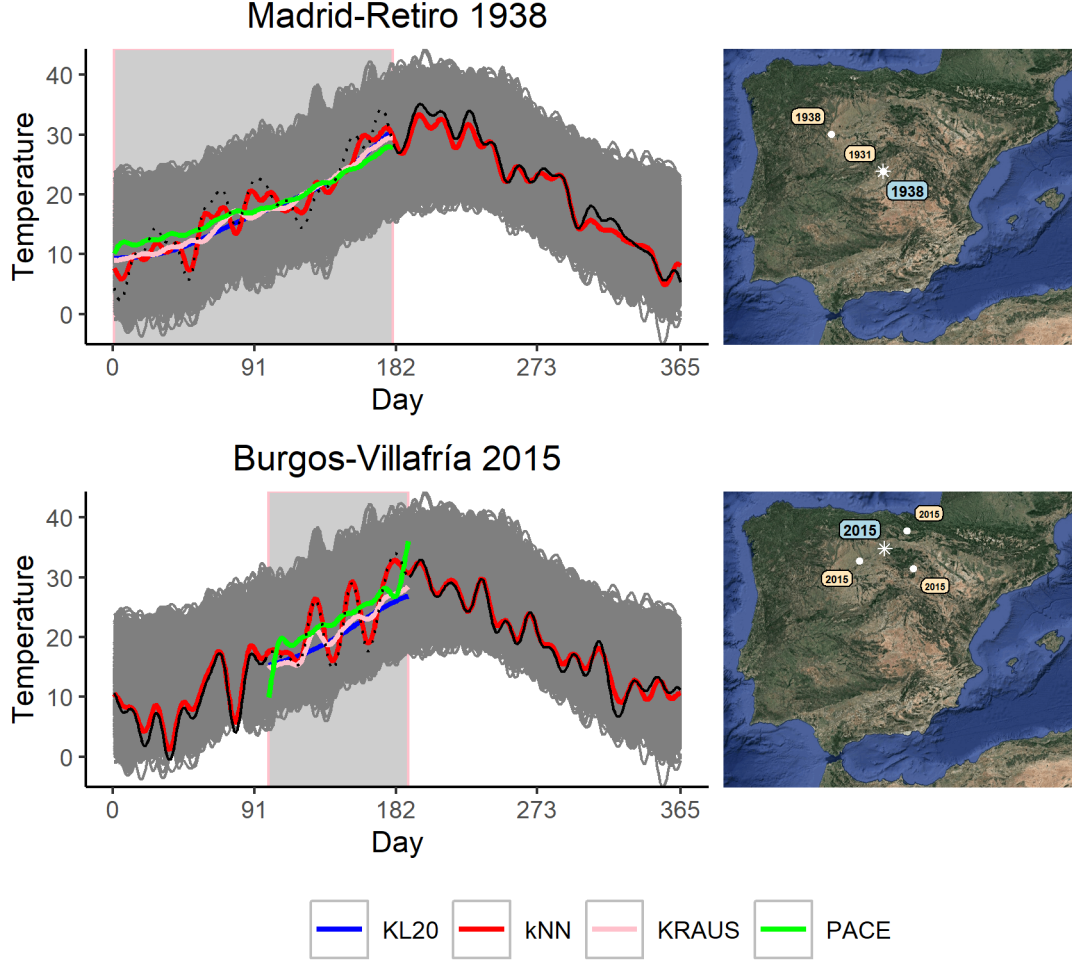


Figure 3: Two illustrations of performance. The randomly observed part of the reconstructed curve is plotted as a black solid line whereas the censored part is dotted. We show both spatial and temporal location of the curves used for reconstruction by  $k$ NN. For reconstructing Madrid-Retiro 1938, the method chose  $k = 2$ , with Zamora 1938 being the 1st NN and Madrid-Retiro 1931 being the 2nd NN. For reconstructing Burgos-Villafria 2015, the method chose  $k = 3$ , with Palencia-Autilla Pino 2015 being the 1st NN, Foronda-Txokiza 2015 the 2nd NN, and Soria 2015 the 3th NN.

## 4 Classification and outlier detection

First we focus on the standard classification problem. Assume that each curve  $X_i$  comes from one of  $G$  groups (subpopulations). Let  $Y_i$  be the group label of  $X_i$ . That is to say  $Y_i$  equals  $y$  if  $X_i$  comes from group  $y$ ,  $1 \leq y \leq G$ . Given the *training sample*  $\{(X_i, Y_i)\}_{i=1}^n$  and a new curve  $X$ , the problem consists of predicting the label  $Y$  of  $X$ . An *ordinary* classifier is a rule that assigns to  $X$  a group label  $m(X)$ . Instead of outputting a group that  $X$  should belong to, a *probabilistic* classifier is a prediction of the conditional probability distribution of  $Y$ .



There exists a wide variety of methods for classifying functional data (Wang et al., 2016). Beyond treating the functional data as simple multivariate data in high dimensional spaces, many of these techniques make use of the fact that they are functions. For example this is done by adding their derivatives, integrals, and/or other preprocessing functions to the analysis (Hubert et al., 2017). The functional  $k$ NN classifier (fkNN) is a straightforward extension of the multivariate rule. In a nutshell, one considers the  $k$  nearest neighbors to the target curve and classifies it with the more represented group. This is the group to which the largest number of the  $k$  nearest neighbors belong. Then  $k$  is chosen to minimize the empirical misclassification rate on the training sample. The method introduced below is inspired by fkNN but differs from it in that the approach is probabilistic.

Let  $I_y$  be the set of indexes  $1 \leq i \leq n$  for which  $Y_i = y$ . Let  $t_1, t_2, \dots, t_M$  be the time points at which the data are observed. Although in practice they often come from a regular grid, formally these times correspond to a realization of a homogeneous Poisson point process on  $[0, 1]$ . Consider the empirical localization distance between  $X$  and the group  $y$ . This is

$$L_y(X) := \frac{1}{M} \sum_{r=1}^M L^{(k)}(X(t_r), \{X_j(t_r), j \in I_y\}). \quad (21)$$

Consider also its mean and variance

$$\mu_y = \frac{1}{M} \sum_{r=1}^M \mathbb{E}[L^{(k)}(X(t_r), \{X_j(t_r), j \in I_y\})] \quad \text{and} \quad \sigma_y^2 = \text{Var}[L_y(X)]. \quad (22)$$

And finally, consider the standardized score  $\tau(X, y) = (L_y(X) - \mu_y)/\sigma_y$ . Denote by  $T$  the random variable  $T = \tau(X, Y)$ . We remark that  $T$  not only depends on  $(X, Y)$  but also on the training  $\{(X_i, Y_i)\}_{i=1}^n$ . Under absolute continuity assumptions on  $T$ , the Bayes rule implies

$$\mathbb{P}(Y = y|T) = \frac{\pi_y f_y(T)}{\sum_{g=1}^G \pi_g f_g(T)},$$

where  $\pi_y = \mathbb{P}(Y = y)$  and  $f_y$  denotes the probability density function of  $T$  conditional on  $\{Y = y\}$ . In such a case, we can consider the so-called Bayes classifier

$$\begin{aligned} m^{(k)}(X) &= \arg \max_y \mathbb{P}(Y = y|T) \\ &= \arg \max_y \pi_y f_y(T). \end{aligned} \quad (23)$$

Note that Theorem 2.4 implies that the conditional distribution of  $T$  given  $\{Y = y\}$ , i.e. the distribution of  $\tau(X, y)$ , can be approximated by a standard normal distribution when  $M$  is large. Therefore, under uniform convergence assumptions, one might expect that  $f_y$  should be approximated by a standard normal density, denoted here by  $\phi$ . For such a reason, it is quite natural to consider, as a practical alternative to the Bayes classifier (23), the classifier

$$\begin{aligned} \tilde{m}^{(k)}(X) &= \arg \max_y \pi_y \phi(\tau(X, y)) \\ &= \arg \max_y \pi_y \phi((L_y(X) - \mu_y)/\sigma_y). \end{aligned} \quad (24)$$

For this, we require knowledge of  $\mu_y$  and  $\sigma_y$ . These values can be estimated from the training as follows. First, consider the empirical localization distance between  $X_i$  and its group  $Y_i$ . According to (21), this is

$$L_i = \frac{1}{M} \sum_{r=1}^M L^{(k)}(X_i(t_r), \{X_j(t_r), j \in I_{Y_i}\}).$$

Next, consider the sample mean and variance of the empirical localization distances for each group. They are

$$\bar{L}_y = \frac{1}{n_y} \sum_{i=1}^n L_i \mathbb{I}_{\{Y_i=y\}} \quad \text{and} \quad S_y^2 = \frac{1}{n_y - 1} \sum_{i=1}^n (L_i - \bar{L}_y)^2 \mathbb{I}_{\{Y_i=y\}}. \quad (25)$$

These are empirical estimators of  $\mu_y$  and  $\sigma_y^2$  in (22). Thus, by plugging these estimators into (24), we obtain the empirical classifier

$$\eta^{(k)}(X) = \arg \max_y \pi_y \phi((L_y(X) - \bar{L}_y)/S_y).$$

If  $M$  is large and  $n_y$  is also large for any group label  $y$ , we expect that  $\eta^{(k)}(X)$  is similar to the Bayes classifier  $m^{(k)}(X)$ . Indeed, what we expect is

$$\mathbb{P}(Y = y|T) \approx \frac{\pi_y \phi((L_y(X) - \bar{L}_y)/S_y)}{\sum_{g=1}^G \pi_g \phi((L_g(X) - \bar{L}_g)/S_g)}.$$

We remark that, although the local feature of the empirical localization distances makes them robust in the presence of outliers, this is not the case of the sample mean and variance in (25). The accuracy of these estimators may be clearly affected by the presence of outlier data. For these reasons we consider trimmed means and variance, by discarding the outliers of each group, when calculating  $\bar{L}_y$  and  $S_y^2$  in (25). The problem of outlier detection in a group, let us say it is  $y$ , is tackled by considering standard boxplots of the samples of empirical localization distances  $\{L_i : Y_i = y\}$ . This tool is simple but powerful given the asymptotic Gaussianity of the empirical localization distances. The problem of outlier detection in the complete population sample is addressed in a similar way by considering only one group.

If two or more groups are similar both in shape and scale, making the classification difficult, then different  $k$  values may provide different labels. The same occurs when one applies  $fk$ NN: different nearest neighbors may belong to different groups. In line with  $fk$ NN, we classify according to the more represented group. In our case, we use the modal label  $\eta^{(1)}(X), \dots, \eta^{(k)}(X)$ . Also, as with  $fk$ NN, the  $k$  value is chosen to minimize the empirical misclassification rate on the training sample. We refer to this classification method by the Localization Classifier, or LC for short.

In order to evaluate the proposed methodology we performed a comparative study with benchmark methods for both outlier detection and classification.

## 4.1 Classification study

We compare  $fkNN$  and LC with two types of functional classifiers. On the one hand, we consider functional extensions of the Depth-to-Depth classifier (DD) (Li et al., 2012) and on the other hand, we consider the classifiers introduced by Hubert et al. (2017), which also are inspired on DD but are based on special distances introduced by the authors instead of depths. Both approaches map functions to points on the plane that require classifying by some bivariate classifier such as  $kNN$ . The theory and methods for the former are discussed by Cuesta-Albertos et al. (2017) whereas Febrero-Bande and Oviedo (2012) developed the corresponding R package. The R package related to the classifiers introduced by Hubert et al. (2017) is also available at The Comprehensive R Archive Network (Segaert et al., 2019). Following these authors, we used  $kNN$  for bivariate classification; both  $kNN$  and  $fkNN$  were based on  $L^2$ -distances. For each methodology we considered the three classifiers suggested by their authors, corresponding to different choices of depth and distance. They are:

1. DD\_hM, DD\_FM and DD\_MBD (Cuesta-Albertos et al., 2017).
2. fAO, fBD and fSD (Hubert et al., 2017).

We tested the eight methods under consideration on the following three examples considered in the literature to which we have referred:

1. The fighter plane dataset used by Hubert et al. (2017). These are 210 univariate functions obtained from digital pictures of seven types of fighter planes, 30 from each type.
2. Second derivative of fat absorbance from the *Tecator* data set used by Cuesta-Albertos et al. (2017). For each piece of finely chopped meat we observe one spectrometric curve which corresponds to the absorbance measured at 100 wavelengths. The pieces are classified according to Ferraty and Vieu (2006) into two classes: with small and large fat content. There are 12 pieces with low content and 103 with high.
3. First derivative of the *Berkeley growth study*. This dataset contains the heights of 39 boys and 54 girls from ages 1 to 18 and is a classic in the literature of FDA (Ramsay and Silverman, 2005).

Complete descriptions of the datasets appear in Cuesta-Albertos et al. (2017) and Hubert et al. (2017). From each group of these datasets, we randomly selected a half of the data for training sample and we classified the rest. We repeated this process one thousand times and reported the missed classification rates on boxplots in Figure 4.

In summary, although all the methods perform well for the plane dataset, the methods of Hubert et al. (2017) were superior for these particular data. Larger misclassifications rates were observed for the other two datasets, where  $fkNN$  was the best option, closely followed by

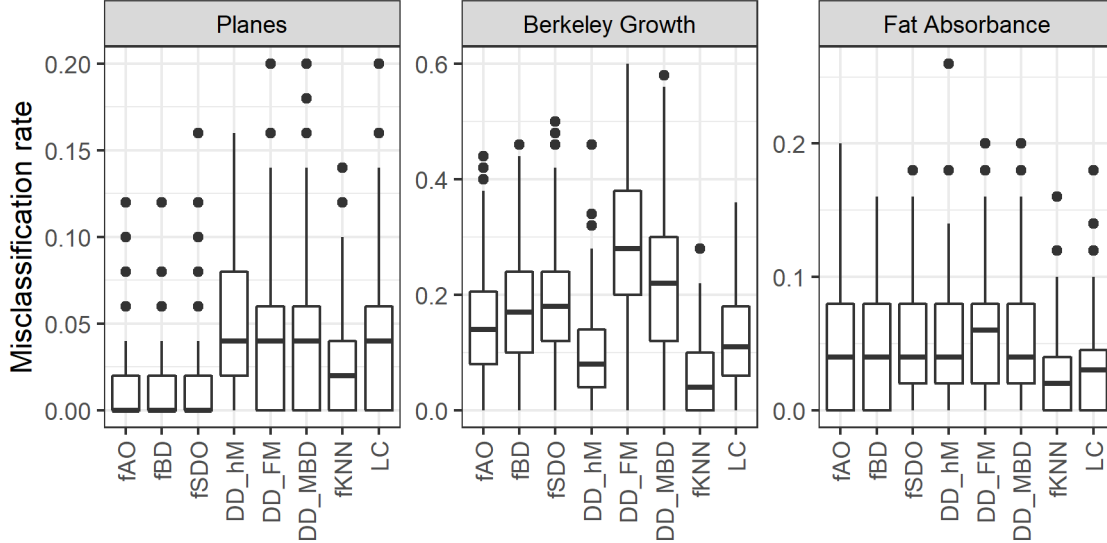


Figure 4: Misclassification rates from 1000 runs.

LC. Only DD\_hM was competitive with LC but at the cost of a long computational running time. The pair ( $k$ NN, LC) offers a good classification tool, combining the efficient ordinary classification by  $k$ NN with the predicted probability provided by LC.

## 4.2 Outlier detection

One of the more popular tools for functional outlier detection is the functional boxplot (Sun and Genton, 2011). This method mimics the univariate boxplot by ordering the sample curves from the ‘median’ outward according to the modified band depth (López-Pintado and Romo, 2009). It is well known that the functional boxplot detects magnitude outliers. These are curves that are outlying in part the observation domain. However, the plot does not necessarily detect shape outliers. They are sample functions that have different shapes from the bulk of data. The outliergram (Arribas-Gil and Romo, 2014) and the MS-plot (Dai and Genton, 2018, 2019) were introduced for tackling both magnitude and shape outliers.

We compare the above three methods with the method based on localization distances. For this, we consider the Japanese mortality dataset discussed in Section 3. For each prefecture we computed the average of the age-specific mortality rates between 1975 and 2007. We only used data until 2007 because data from the Saitama prefecture is not available after this date. In this way, we obtain 47 mortality curves smoothed by averaging corresponding to each prefecture. Using the default parameters suggested by the authors, all the methods detected an outlier at Okinawa, where residents have famously lived longer than anywhere else in the world. In addition, the outliergram also detected outliers at Fukui and Kochi. Indeed, we observe that the curves corresponding to these two prefectures exhibit strong oscillations for ages below

fifty years. These oscillations are not seen in the greater part of the prefectures, which have smoother curves. Regarding localization distances, the boxplots corresponding to Okinawa and Aomori were very extreme outliers for all the considered  $k$  values. We remark that, although the rest of the methods did not detect an outlier at Aomori, this prefecture has experienced the highest mortality rates for many years. In fact, Aomori has been already considered an outlier by Japanese health officials (O'Donoghue, 2019). For several values of  $k$ , the localization distances corresponding to Fukui, Kochi and Tokyo fell above the default whiskers of the corresponding boxplots. Indeed, we observe that Tokyo is a deep datum for ages above thirty years but it has extreme low values of mortality rates for ages below 25. Finally, only for a few values of  $k$ , Nagano, Shiga and Kanagawa provide outliers with localization distances and they fell close to the default whiskers. In fact, by considering the more conservative upper whisker ( $Q_3 + 3 * IQR$  instead  $Q_3 + 1.5 * IQR$ ) neither Tokyo, Nagano, Shiga nor Kanagawa would be considered as outliers. However, it is interesting to observe that both Nagano and Shiga show shapes similar to Fukui and Kochi, although with more moderate oscillations. Also, the behavior of Kanagawa is similar to Tokyo, but with less extreme mortality rates for ages below 25. The only value for which the eight mentioned prefectures fall above of the default whiskers is  $k = 9$ . All the above can be observed from Figures 5 and 6. In the former, we plot the outputs of all the methods under consideration. In the latter, we show the particular case  $k = 9$ , where the reader can inspect the curve of each prefecture under consideration.

In conclusion, though localization distance statistics agreed with the three benchmark methods with respect to Okinawa and with the outliergram for Fukui and Kochi, they recognize Okinawa as an extreme outlier. In addition, the localization distances were able to detect Aomori as an extreme outlier and indicate a certain atypicality of Tokyo. Also, they drew attention to a small departure from the bulk of prefectures of Nagano, Shiga and Kanagawa.

## 5 Discussion

The localization processes introduced here (1) are an alternative way to approximate curves from a given functional sample. These processes can be seen as piecewise approximations of different orders to a function from data collected in a functional setting. Other estimation methods, for example those based on functional  $k$ NN and model-generated curves, often consider distances on function spaces for measuring nearness. Unlike these methods, we consider the so-called localization distance process formed by the point-by-point distances between the target curve and its corresponding approximation. Beyond the interest per se of these processes, we introduce them in to provide a foundation for the rigorous asymptotic theory of functional estimation.

First, we provide weak laws for localization distances when the number of sample curves increases up to infinity. These results allow one to elucidate mild assumptions under which

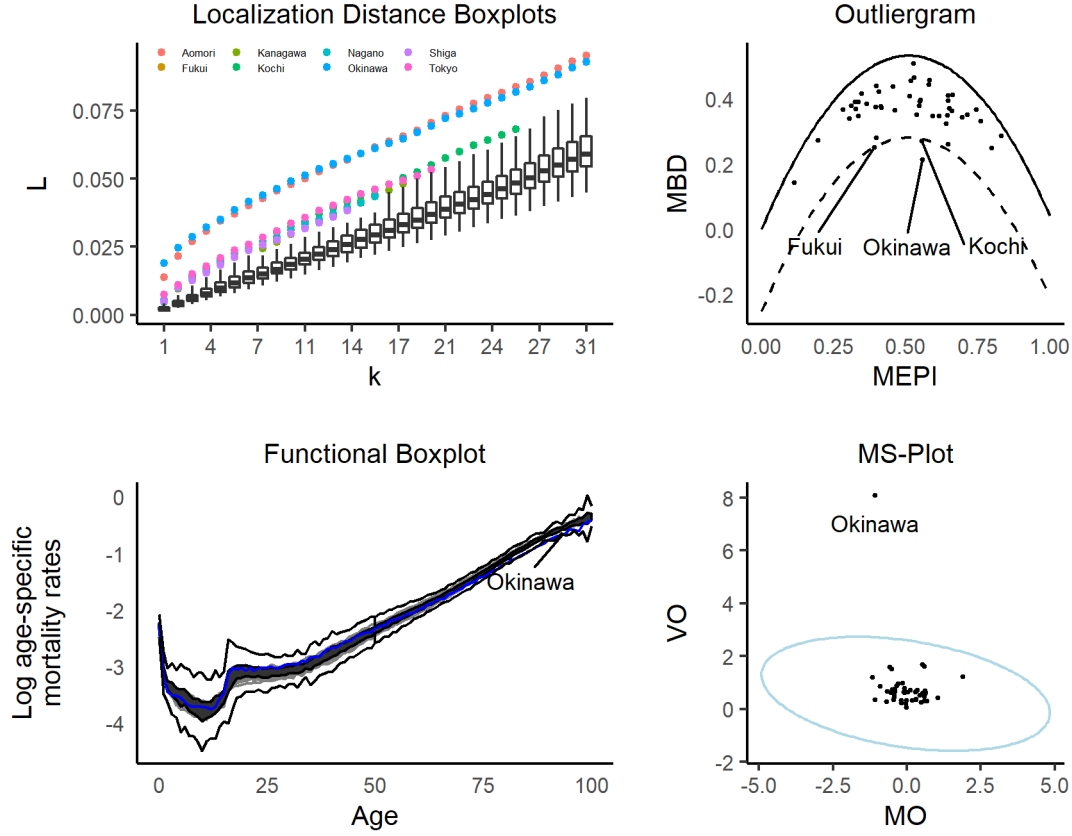


Figure 5: Outputs from the outlier detection methods under consideration. All the methods detect Okinawa. Outliergram and localization distance boxplots agree with respect to Fukui and Kochi. The localization distances are the only ones able to detect Aomori as an extreme outlier and the only ones indicating a certain atypicality of Tokyo. For a few values of  $k$ , the localization distances corresponding to Nagano, Shiga and Kanagawa fell above (but close) to the default whiskers.

nearby neighbors to a target function on an observable range remain near the target outside this range. This property is the key to proving consistency of  $k$ NN type estimators for reconstructing curves from partially observed data. A particular  $k$ NN methodology is introduced and compared with three benchmark methods. We present results of a simulation study based on yearly curves of daily Spanish temperatures and Japanese age-specific mortality rates, two real world examples where a large range of contiguous data is missing, but which may be reconstructed. Beyond the intuitive appeal of the method, the results are promising in terms of accuracy, computational efficiency, and interpretability.

Second, we establish asymptotic normality for averages of localization distances by considering different settings in which the number of sample curves is large enough. The results provide rates of convergence for the point-estimation average error of the  $k$ NN method and their

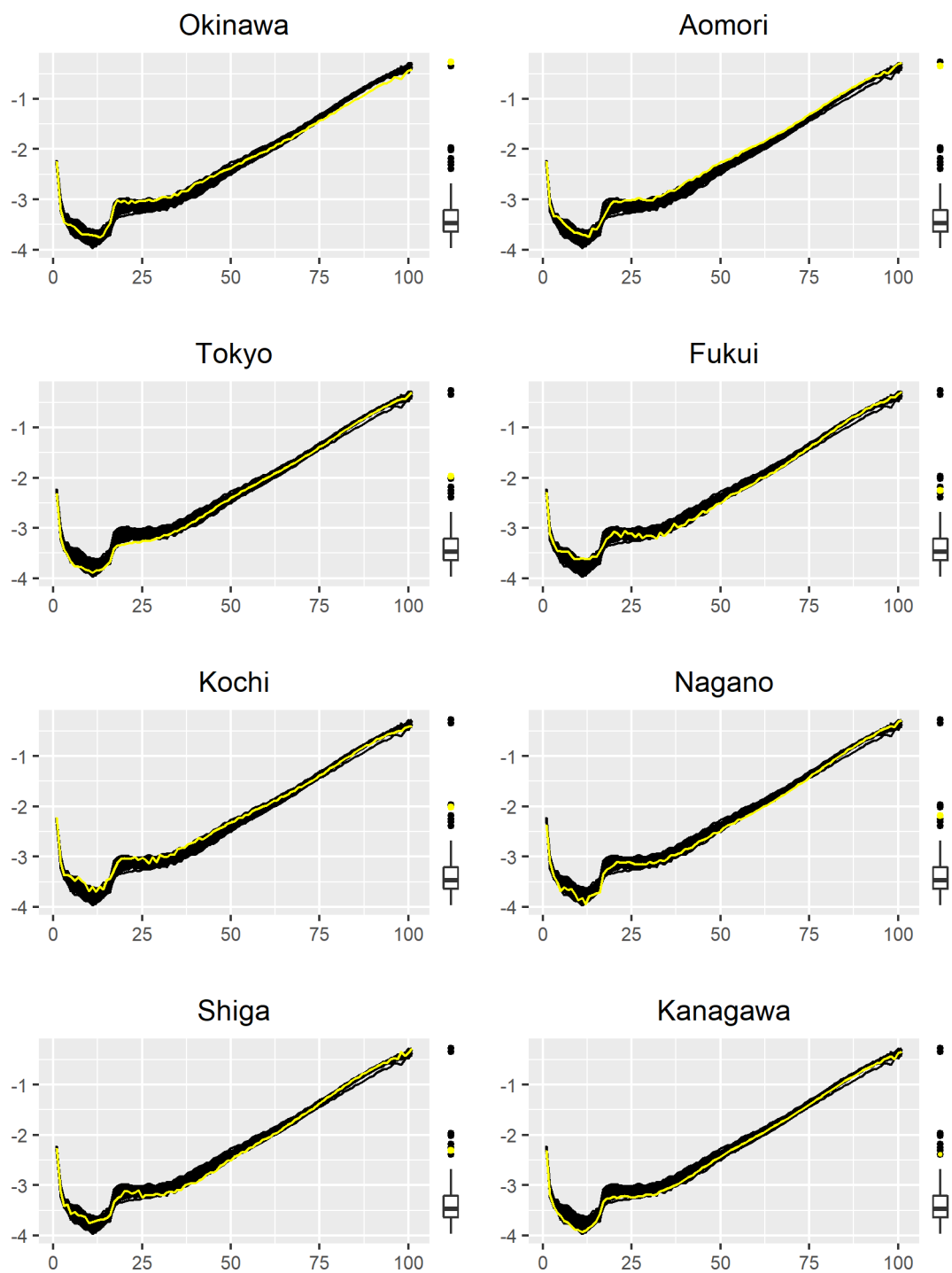


Figure 6: Log age-specific mortality rates and localization distances boxplot for  $k = 9$ . Each outlier value and its corresponding curve are highlighted in yellow.

variance when both the number of unobserved data and the number of observed data is large at an observation time  $t$ ; such results distinguish the  $k$ NN method from other reconstruction methods.

Third, we obtain central limit theorems for empirical localization distances that form the basis of new methods for classification as well as outlier detection. These are problems where the  $k$ NN approach has been widely considered. The comparative study shows that the classification method proposed here is competitive with several benchmark methods. Only  $k$ NN gave consistently superior results. However, the new method predicts classification probabilities and provides standard normal scores that help validate the outputs rather than to only generate them. This makes the method a useful complementary tool capable of providing probabilistic support to the ordinary  $k$ NN classification. Regarding outlier detection, the case study considered shows that the method based on localization distances can detect both magnitude and shape outliers that other methods do not.

In conclusion, we emphasize that the dual purpose of this paper has been to not only introduce the  $k$ NN localization processes and their associated  $k$ NN localization distances, but to also provide useful mathematical tools lending rigor to both the current approach and possible further approximation schemes based on nearest neighbors. In particular, there remains the potential for further exploiting the asymptotic first and second order properties of stabilizing localization distances in functional data analysis.

## 6 Proofs of results in Section 2

### 6.1 Proof of Theorem 2.1

(i) We first prove (3). Let  $t \in [0, 1]$  be such that the marginal density  $\kappa_t$  exists. By translation invariance of  $W_n^{(k)}$  we have

$$\begin{aligned} \mathbb{E}W_n^{(k)}(X_1(t), \{X_j(t)\}_{j=1}^n) &= \mathbb{E}L^{(k)}\left(\frac{2n}{k \cdot |S(\kappa_t)|} |X_1(t), \frac{2n}{k|S(\kappa_t)|} \{X_j(t)\}_{j=1}^n\right) \\ &= \frac{2}{k|S(\kappa_t)|} \mathbb{E}L^{(k)}(\mathbf{0}, n(\{X_j(t)\}_{j=1}^n - X_1(t))) \\ &\rightarrow \int_{S(\kappa_t)} \frac{2}{k|S(\kappa_t)|} \mathbb{E}L^{(k)}(\mathbf{0}, \mathcal{P}_{\kappa_t(y)}) \kappa_t(y) dy, \end{aligned}$$

where the limit as  $n \rightarrow \infty$  follows since  $L^{(k)}$  is a stabilizing score function and where we use Theorem 2.1 of Penrose and Yukich (2003). Now for any constant  $\tau$  we have  $\mathbb{E}L^{(k)}(\mathbf{0}, \mathcal{P}_\tau) = \tau^{-1} \mathbb{E}L^{(k)}(\mathbf{0}, \mathcal{P}_1)$ . Notice that  $L^{(k)}(\mathbf{0}, \mathcal{P}_1)$  is a Gamma  $\Gamma(k, 2)$  random variable with shape parameter  $k$  and scale parameter 2 and thus  $\mathbb{E}L^{(k)}(\mathbf{0}, \mathcal{P}_1) = k/2$ . The proof of (3) is complete.

(ii) To prove (4), we replace  $W_n^{(k)}(X_1(t), \{X_j(t)\}_{j=1}^n)$  by its square in the above computation. Also, for any constant  $\tau$  we have  $\mathbb{E}(W^{(k)}(\mathbf{0}, \mathcal{P}_\tau))^2 = \tau^{-2} \mathbb{E}(L^{(k)}(\mathbf{0}, \mathcal{P}_1))^2 = \tau^{-2}(k+1)k/4$ , since



the second moment of a Gamma  $\Gamma(k, 2)$  random variable equals  $(k + 1)k/4$ . These facts yield (4).

(iii) The limit (5) follows because  $L^{(k)}$  is a stabilizing score function and thus as  $n \rightarrow \infty$

$$\begin{aligned} W_n^{(k)}(X_1(t), \{X_j(t)\}_{j=1}^n) &= \frac{2}{k|S(\kappa_t)|} L^{(k)}(\mathbf{0}, n(\{X_j(t)\}_{j=1}^n - X_1(t))) \\ &\xrightarrow{\mathcal{D}} \frac{2}{k|S(\kappa_t)|} L^{(k)}(\mathbf{0}, \mathcal{P}_{\kappa_t}(X_1(t))). \end{aligned}$$

See Penrose and Yukich (2003), section 3 and Penrose (2007b).  $\square$

## 6.2 Proof of Theorem 2.2

(i) Fix  $\alpha \in (0, 1]$ . Let  $t \in [0, 1]$  be such that the marginal density  $\kappa_t$  exists. For each  $y \in S(\kappa_t)$ , we may couple the point process  $n(\mathcal{P}_{n\kappa_t} - y)$  with the homogenous Poisson point process  $\mathcal{P}_{\kappa_t}(y)$  in such a way that the probability that the two point processes are not equal on  $[-A, A]$  is bounded by

$$\int_{-A}^A |\kappa_t\left(\frac{x}{n} + y\right) - \kappa_t(y)| dx \leq 2A \left(\frac{A}{n}\right)^\alpha. \quad (26)$$

We will need this coupling in what follows.

Recall that  $N(n)$  is a Poisson random variable with parameter  $n$ . Write  $k$  instead of  $k(n)$ . As  $n \rightarrow \infty$  we have by translation invariance of  $W_n^{(k)}$

$$\begin{aligned} \mathbb{E}W_n^{(k)}(X_1(t), \{X_j(t)\}_{j=1}^{N(n)}) &= \mathbb{E}L^{(k)}\left(\frac{2n}{k|S(\kappa_t)|}X_1(t), \frac{2n}{k|S(\kappa_t)|}\{X_j(t)\}_{j=1}^{N(n)}\right) \\ &= \frac{2}{k|S(\kappa_t)|} \mathbb{E}L^{(k)}(\mathbf{0}, n(\{X_j(t)\}_{j=1}^{N(n)} - X_1(t))). \end{aligned}$$

Define the event that the scaled width around a point inserted at the origin is determined by data within distance  $c(k + \log n)$  of the origin, namely

$$E_n := \{L^{(k)}(\mathbf{0}, n(\{X_j(t)\}_{j=1}^{N(n)} - X_1(t))) \cap B_{c(k+\log n)}(\mathbf{0}) = L^{(k)}(\mathbf{0}, n(\{X_j(t)\}_{j=1}^{N(n)} - X_1(t)))\}.$$

Here  $B_{c(k+\log n)}(\mathbf{0})$  is the ball centered at the origin of radius  $c(k + \log n)$ . The event  $E_n^c$  is the event that the cardinality of  $n(\{X_j(t)\}_{j=1}^{N(n)} - X_1(t)) \cap B_{c(k+\log n)}(\mathbf{0})$  is less than  $k$ . This is the event that a Poisson random variable with parameter  $c(k + \log n)$  is less than  $k$ . By standard deviation estimates for Poisson random variables, the probability of this event decays exponentially fast in  $c \log n$ . Thus, if the constant  $c$  is large enough, then  $\mathbb{P}(E_n^c)$  can be made smaller than any power of  $n$ .

Now write

$$\begin{aligned}
& \frac{2}{k|S(\kappa_t)|} \mathbb{E} L^{(k)}(\mathbf{0}, n(\{X_j(t)\}_{j=1}^{N(n)} - X_1(t))) \\
&= \frac{2}{k|S(\kappa_t)|} \mathbb{E} L^{(k)}(\mathbf{0}, n(\{X_j(t)\}_{j=1}^{N(n)} - X_1(t))) \mathbf{1}(E_n) \\
&\quad + \frac{2}{k|S(\kappa_t)|} \mathbb{E} L^{(k)}(\mathbf{0}, n(\{X_j(t)\}_{j=1}^{N(n)} - X_1(t))) \mathbf{1}(E_n^c).
\end{aligned}$$

Choosing  $c$  large enough, we find that the last term on the right-hand side goes to zero as  $n \rightarrow \infty$ . We use the coupling (26) to show that the first term converges to 1 as  $n \rightarrow \infty$ . We first write

$$\begin{aligned}
& \frac{2}{k|S(\kappa_t)|} \mathbb{E} L^{(k)}(\mathbf{0}, n(\{X_j(t)\}_{j=1}^{N(n)} - X_1(t))) \mathbf{1}(E_n) \\
&= \frac{2}{k|S(\kappa_t)|} \int_{S(\kappa_t)} \mathbb{E} L^{(k)}(\mathbf{0}, n(\{X_j(t)\}_{j=1}^{N(n)} - y)) \mathbf{1}(E_n) \kappa_t(y) dy.
\end{aligned}$$

The point set  $n(\{X_j(t)\}_{j=1}^{N(n)} - y)$  is the scaled point process  $n(\mathcal{P}_{n\kappa_t} - y)$  and has intensity density  $\kappa_t(\frac{x}{n} + y)$ ,  $x \in -n(S(\kappa_t) - y)$ . By coupling (26), the event  $F_n$  that this point set is not equal to the Poisson point process  $\mathcal{P}_{\kappa_t(y)}$  on the ball  $B_{c(k+\log n)}(\mathbf{0})$  satisfies the probability bound  $\mathbb{P}(F_n) \leq 2A(A/n)^\alpha$ , where  $A = c(k + \log n)$ . Thus, as  $n \rightarrow \infty$

$$\left| \frac{2}{k|S(\kappa_t)|} \left( \mathbb{E} L^{(k)}(\mathbf{0}, n(\{X_j(t)\}_{j=1}^{N(n)} - y)) \mathbf{1}(E_n) \kappa_t(y) - \mathbb{E} L^{(k)}(\mathbf{0}, \mathcal{P}_{\kappa_t(y)}) \mathbf{1}(E_n) \kappa_t(y) \right) \right| \rightarrow 0$$

for all  $y \in S(\kappa_t)$ . Here we have used the Cauchy-Schwarz inequality and  $\lim_{n \rightarrow \infty} k^{1+\alpha}/n^\alpha = 0$  to obtain the intermediate step

$$\frac{1}{k} \mathbb{E} L^{(k)}(\mathbf{0}, n(\{X_j(t)\}_{j=1}^{N(n)} - y)) \mathbf{1}(E_n) \mathbf{1}(F_n) \leq \frac{(ck^2)^{1/2}}{k} \mathbb{P}(F_n)^{1/2} \rightarrow 0,$$

with a similar bound for  $\frac{1}{k} \mathbb{E} L^{(k)}(\mathbf{0}, \mathcal{P}_{\kappa_t(y)}) \mathbf{1}(E_n) \mathbf{1}(F_n)$ . The proof of (6) is complete since

$$\lim_{n \rightarrow \infty} \frac{2}{k|S(\kappa_t)|} \int_{S(\kappa_t)} \mathbb{E} L^{(k)}(\mathbf{0}, \mathcal{P}_{\kappa_t(y)}) \mathbf{1}(E_n) \kappa_t(y) dy = 1.$$

(ii) The limit (7) follows by replacing  $W_n^{(k)}(X_1(t), \{X_j(t)\}_{j=1}^{N(n)})$  by its square in the above computation. Also, for any constant  $\tau$  we have  $\mathbb{E}(L^{(k)}(\mathbf{0}, \mathcal{P}_\tau))^2 = \tau^{-2} \mathbb{E}(L^{(k)}(\mathbf{0}, \mathcal{P}_1))^2 = \tau^{-2}(k+1)k/4$ , since the second moment of a Gamma(k,2) random variable equals  $(k+1)k/4$ .  $\square$

### 6.3 Proof of Theorem 2.3

The next result gives a rate of convergence of mean distances. While it is of independent interest, we will use it in the proof of Theorem 2.3.

**Proposition 2.** (rate of convergence of expected width on Poisson input and marked Poisson input) Assume  $t \in [0, 1]$  is such that  $\kappa_t$  exists and satisfies the conditions of Theorem 2.3. For all  $k = 1, 2, \dots$  there is a constant  $c(k)$  such that

$$\left| \mathbb{E}W_n^{(k)}(X_1(t), \{X_j(t)\}_{j=1}^{N(n)}) - 1 \right| \leq \frac{c(k)}{n}, \quad n \geq 1. \quad (27)$$

Also, on the event  $\{i \in I_0(t)\}$  we have

$$\left| \mathbb{E}W_n^{(k)}(\tilde{X}_i(t), \{\tilde{X}_j(t)\}_{j=1}^{N(n)}) - \frac{1}{1-p} \right| \leq \frac{c(k)}{n}, \quad n \geq 1. \quad (28)$$

*Proof.* We prove (27) as (28) follows from identical methods. We write  $\{X_j(t)\}_{j=1}^{N(n)}$  as a Poisson point process  $\mathcal{P}_{n\kappa_t}$  having intensity  $n\kappa_t$  on  $S(\kappa_t)$ . By the Mecke formula we have

$$\mathbb{E}W_n^{(k)}(X_1(t), \{X_j(t)\}_{j=1}^{N(n)}) = \int_{S(\kappa_t)} \mathbb{E}W_n^{(k)}(x, \mathcal{P}_{n\kappa_t}) \kappa_t(x) dx. \quad (29)$$

We let  $\mathcal{P}_\tau$  be a Poisson point process on  $\mathbb{R}$  of intensity  $\tau$ . We have  $1 = \frac{2}{k} \mathbb{E}L^{(k)}(\mathbf{0}, \mathcal{P}_1) = \frac{2}{k} \mathbb{E}L^{(k)}(x, \mathcal{P}_1) = \frac{2n}{k} \mathbb{E}L^{(k)}(x, \mathcal{P}_{n\kappa_t(x)}) \kappa_t(x)$  since  $n\tau \mathcal{P}_{n\tau} \stackrel{\mathcal{D}}{=} \mathcal{P}_1$  for all  $n \geq 1$  and all  $\tau \in (0, \infty)$ . Thus

$$\mathbb{E}[W_n^{(k)}(x, \mathcal{P}_{n\kappa_t(x)})] \kappa_t(x) = \frac{1}{|S(\kappa_t)|}.$$

Thus, integrating over all  $x \in S(\kappa_t)$  gives

$$1 = \int_{S(\kappa_t)} \mathbb{E}[W_n^{(k)}(x, \mathcal{P}_{n\kappa_t(x)})] \kappa_t(x) dx. \quad (30)$$

Combining (29) and (30) we get

$$\begin{aligned} & \left| \mathbb{E}W_n^{(k)}(X_1(t), \{X_j(t)\}_{j=1}^{N(n)}) - 1 \right| \\ & \leq \int_{S(\kappa_t)} \left| \mathbb{E}W_n^{(k)}(x, \mathcal{P}_{n\kappa_t}) - \mathbb{E}W_n^{(k)}(x, \mathcal{P}_{n\kappa_t(x)}) \right| \kappa_t(x) dx. \end{aligned}$$

Coupling arguments similar to those in the Appendix of Schulte and Yukich (2020) show that there is a constant  $c(k)$  such that for all  $x \in S(\kappa_t)$

$$\left| \mathbb{E}W_n^{(k)}(x, \mathcal{P}_{n\kappa_t}) - \mathbb{E}W_n^{(k)}(x, \mathcal{P}_{n\kappa_t(x)}) \right| \leq c[n^{-1} + \exp(-cn\mathbf{d}(x, \partial(S(\kappa_t))))],$$

where  $\mathbf{d}(x, \partial(S(\kappa_t)))$  stands for the distance between  $x$  and the boundary of  $S(\kappa_t)$ . Combining the last two displays gives

$$\left| \mathbb{E}W_n^{(k)}(X_1(t), \{X_j(t)\}_{j=1}^{N(n)}) - 1 \right| \leq c \int_{S(\kappa_t)} [n^{-1} + \exp(-cn\mathbf{d}(x, \partial(S(\kappa_t))))] \kappa_t(x) dx.$$

Making a change of variable gives the desired result.  $\square$

Now we are ready to give the proof of Theorem 2.3.

*Proof.* We first establish the asymptotic normality assertions. To establish (9) we first show as  $n \rightarrow \infty$

$$\frac{\sum_{i \in I_0(t)} \left( W_n^{(k)} \left( \tilde{X}_i(t), \{\tilde{X}_j(t)\}_{j=1}^{N(n)} \right) - \mathbb{E} W_n^{(k)} \left( \tilde{X}_i(t), \{\tilde{X}_j(t)\}_{j=1}^{N(n)} \right) \right)}{\sqrt{n(1-p)}} \xrightarrow{\mathcal{D}} N \left( 0, \nu^2(t, k) \right). \quad (31)$$

The limit (31) is a consequence of general limit theory for sums of exponentially stabilizing functionals on marked Poisson point sets, as given in e.g. Baryshnikov and Yukich (2005) and Penrose (2007a). It suffices to note that the localization distance  $L^{(k)}$  is an exponentially stabilizing score function. This is because its value at a point  $x$  is determined by the spatial locations of the  $k$  nearest neighbors to  $x$  and because the density  $\kappa_t$  is bounded away from zero. Such functionals are known to be stabilizing, see e.g. Lachièze-Rey et al. (2019) and Penrose and Yukich (2003). To deduce (9) from (31) we apply the rate result (28).

We deduce the rate results (11) and (12) from a general result on rates of normal convergence for exponentially stabilizing functionals of marked point processes; see Theorem 2.3(a) of Lachièze-Rey et al. (2019). In particular we make use of the growth bounds  $\text{Var}[\sum_{i=1}^{N(n)} W_n^{(k)}(\tilde{X}_i(t), \{\tilde{X}_j(t)\}_{j=1}^{N(n)})] = \Theta(n)$ , the validity of which is discussed in Remark 2, following Theorem 3.1 in Lachièze-Rey et al. (2019). The lower bound  $\text{Var}[\sum_{i=1}^{N(n)} W_n^{(k)}(\tilde{X}_i(t), \{\tilde{X}_j(t)\}_{j=1}^{N(n)})] = \Omega(n)$  insures that

$$d_K \left( \frac{\sum_{i \in I_0(t)} \left( W_n^{(k)} \left( \tilde{X}_i(t), \{\tilde{X}_j(t)\}_{j=1}^{N(n)} \right) - \mathbb{E} W_n^{(k)} \left( \tilde{X}_i(t), \{\tilde{X}_j(t)\}_{j=1}^{N(n)} \right) \right)}{\sqrt{\text{Var} \sum_{i \in I_0(t)} W_n^{(k)} \left( \tilde{X}_i(t), \{\tilde{X}_j(t)\}_{j=1}^{N(n)} \right)}}, N(0, 1) \right) \leq \frac{C_1(k)}{\sqrt{n}}. \quad (32)$$

The upper bound  $\text{Var}[\sum_{i=1}^{N(n)} W_n^{(k)}(\tilde{X}_i(t), \{\tilde{X}_j(t)\}_{j=1}^{N(n)})] = O(n)$ , along with (28), insure that replacing  $\mathbb{E} W_n^{(k)} \left( \tilde{X}_i(t), \{\tilde{X}_j(t)\}_{j=1}^{N(n)} \right)$  by  $(1-p)^{-1}$  gives an error which is at most  $\frac{C(k)}{\sqrt{n}}$  where  $C(k)$  is a constant which depends on  $k$ . These two remarks give (11). The rate (12) is proved similarly.

The asymptotics (10) may be deduced from general variance asymptotics for sums of exponentially stabilizing score functions on marked Poisson input. We refer the reader to Baryshnikov and Yukich (2005) and also Penrose (2007a). The limit (13) follows since

$$\lim_{n \rightarrow \infty} \frac{\text{Var} \sum_{i \in I_1(t)} W_n^{(k)} \left( \tilde{X}_i(t), \{\tilde{X}_j(t)\}_{j=1}^{N(n)} \right)}{np} = \frac{4\tilde{\sigma}_t^2}{(1-p)^2 k^2}.$$

This completes the proof of Theorem 2.3.  $\square$

## Acknowledgements

The research of J. Yukich is supported in part by a Simons collaboration grant. He is also grateful for generous support from the Department of Statistics at Universidad Carlos III de Madrid, where this research was completed.

# References

- Arribas-Gil, A. and Romo, J. (2014). Shape outlier detection and visualization for functional data: the outliergram. *Biostatistics*, 15(4):603–619.
- Baryshnikov, Y. and Yukich, J. E. (2005). Gaussian limits for random measures in geometric probability. *Ann. Appl. Probab.*, 15:213–253.
- Biau, B., C  rou, F., and Guyader, A. (2010). Rates of convergence of the functional  $k$ -nearest neighbor estimate. *IEEE Trans. Inform. Theory*, 56:2034–2040.
- Brito, M. R., Ch  vez, E. L., Quiroz, A. J., and Yukich, J. E. (1997). Connectivity of the mutual  $k$ -nearest-neighbor graph in clustering and outlier detection. *Statistics and Probability Letters*, 35:33–42.
- Chen, Y., Carroll, C., Dai, X., Fan, J., P., H., Han, K., Ji, H., Mueller, H.-G., and Wang, J.-L. (2020). *fdapace: Functional Data Analysis and Empirical Dynamics*. R package version 0.5.2. Development version at <https://github.com/functionaldata/tPACE>.
- Cuesta-Albertos, J. A., Febrero-Bande, M., and Oviedo de la Fuente, M. (2017). The  $DD^g$ -classifier in the functional setting. *TEST*, 26(1):119–142.
- Dai, W. and Genton, M. G. (2018). Multivariate functional data visualization and outlier detection. *Journal of Computational & Graphical Statistics*, 27:923–934.
- Dai, W. and Genton, M. G. (2019). Directional outlyingness for multivariate functional data. *Computational Statistics & Data Analysis*, 131:50–65.
- Febrero-Bande, M., Galeano, P., and Gonz  lez-Manteiga, W. (2019). Estimation, imputation and prediction for the functional linear model with scalar response with responses missing at random. *Computational Statistics & Data Analysis*, 131:91–103.
- Febrero-Bande, M. and Oviedo, M. (2012). Statistical computing in functional data analysis: The R package *fda.usc*. *Journal of Statistical Software*, 51(4):1–28.
- Ferraty, F. and Vieu, P. (2006). *Nonparametric functional data analysis*. Springer, New York.
- Gao, Y., Shang, H. L., and Yang, Y. (2019). High-dimensional functional time series forecasting: An application to age-specific mortality rates. *Journal of Multivariate Analysis*, 170:232–243.
- Gy  rfi, L., Kohler, M., Krzyzak, A., and Walk, H. (2002). *A. Distribution-Free Theory of Nonparametric Regression*. Springer, New York.
- Hubert, M., Rousseeuw, P., and Segaeert, P. (2017). Multivariate and functional classification using depth and distance. *Advances in Data Analysis and Classification*, 11:445–466.

- Hyndman, R. J. and Booth, H. (2008). Stochastic population forecasts using functional data models for mortality, fertility and migration. *International Journal of Forecasting*, 24:323–342.
- Hyndman, R. J. and Ullah, S. (2007). Robust forecasting of mortality and fertility rates: a functional data approach. *Computational Statistics & Data Analysis*, 51:4942–4956.
- Kara, L.-Z., Laksaci, A., Rachdi, M., and Vieu, P. (2017). Data-driven  $k$ nn estimation in nonparametric functional data analysis. *Journal of Multivariate Analysis*, 153:176–188.
- Kneip, A. and Liebl, D. (2020). On the optimal reconstruction of partially observed functional data. *Ann. Statistics*, (forthcoming).
- Kraus, D. (2015). Components and completion of partially observed functional data. *Journal of the Royal Statistical Society*, 77:777–801.
- Kudraszow, N. and Vieu, P. (2013). Uniform consistency of  $k$ nn regressors for functional variables. *Statist. Probab. Lett.*, 83:1863–1870.
- Lachière-Rey, R., Schulte, M., and Yukich, J. E. (2019). Normal approximation for stabilizing functionals. *Ann. Appl. Probab.*, 29:931–991.
- Li, J., Cuesta-Albertos, J. A., and Liu, R. Y. (2012). DD-classifier: Nonparametric classification procedure based on DD-plot. *Journal of the American Statistical Association*, 107:737–753.
- Lian, H. (2011). Convergence of functional  $k$ -nearest neighbor regression estimate with functional responses. *Electronic Journal of Statistics*, 5:31–40.
- Liebl, D. (2019). Nonparametric testing for differences in electricity prices: The case of the fukushima nuclear accident. *The Annals of Applied Statistics*, 13:1128–1146.
- López-Pintado, S. and Romo, J. (2009). On the concept of depth for functional data. *Journal of the American Statistical Association*, 104(486):718–734.
- Martínez, F., Frías, M. P., Pérez, M. D., and Rivera, A. J. (2017). A methodology for applying  $k$ -nearest neighbor to time series forecasting. *Artif. Intell. Rev.*, 52:2019–2037.
- O’Donoghue, J. J. (2019). Salt and inaction blamed for Aomori having the lowest life expectancy in Japan. *The Japan Times*. Available at [https://www.japantimes.co.jp/?post\\_type=news&p=2340547](https://www.japantimes.co.jp/?post_type=news&p=2340547).
- Penrose, M. D. (2007a). Gaussian limits for random geometric measures. *Electron. J. Probab.*, 12:989–1035.
- Penrose, M. D. (2007b). Laws of large numbers in stochastic geometry with statistical applications. *Bernoulli*, 13(4):1124–1150.

- Penrose, M. D. and Yukich, J. E. (2001). Central limit theorems for some graphs in computational geometry. *Ann. App. Prob.*, 11:1005–1041.
- Penrose, M. D. and Yukich, J. E. (2003). Weak laws of large numbers in geometric probability. *Ann. Appl. Probab.*, 13:277–303.
- Penrose, M. D. and Yukich, J. E. (2005). *Stein’s Method and Applications, Lecture Note Series, Inst. for Math. Sci., National Univ. Singapore*, volume 5, chapter Normal approximation in geometric probability, pages 37–58. World Scientific.
- Ramaswamy, S., Rastogi, R., and Shim, K. (2000). Efficient algorithms for mining outliers from large data sets. In *Proceedings of the ACM SIGMOD Conference on Management of Data*, pages 427–438.
- Ramsay, J. and Silverman, B. (2005). *Functional Data Analysis*. Springer, New York, 2nd edition.
- Rinott, Y. and Rotar, V. (1996). A multivariate CLT for local dependence with  $n^{-1/2} \log n$  rate and applications to multivariate graph related statistics. *Journal of multivariate analysis*, 56:333–350.
- Schreiber, T. (2010). *New perspectives in stochastic geometry*, chapter Limit theorems in stochastic geometry, pages 111–144. Oxford University Press, Oxford.
- Schulte, M. and Yukich, J. E. (2020). Rates of multivariate normal approximation for statistics in geometric probability. Preprint.
- Segaert, P., Hubert, M., Rousseeuw, P., and Raymaekers, J. (2019). *mrfDepth: Depth Measures in Multivariate, Regression and Functional Settings*. R package version 1.0.11.
- Shang, H. L. and Hyndman, R. J. (2017). Grouped functional time series forecasting: An application to age-specific mortality rates. *Journal of Computational & Graphical Statistics*, 26(2):330–343.
- Sun, Y. and Genton, M. G. (2011). Functional boxplots. *Journal of Computational & Graphical Statistics*, 20:316–334.
- University of California, Berkeley (USA) and Max Planck Institute for Demographic Research (Germany) (2019). Human Mortality Database. Available at [www.mortality.org](http://www.mortality.org).
- Wang, J.-L., Chiou, J.-M., and Müller, H.-G. (2016). Functional data analysis. *Annu. Rev. Stat. Appl.*, 3:257–295.
- Wu, X., Kumar, V., Ross Quinlan, J., Ghosh, J., Yang, Q., Motoda, H., McLachlan, G. J., Ng, A., Liu, B., Yu, P. S., Zhou, Z.-H., Steinbach, M., Hand, D., and Steinberg, D. (2008). Top 10 algorithms in data mining. *Knowl. Inf. Syst.*, 14:1–37.

- Yao, F., Müller, H.-G., and Wang, J.-L. (2005). Functional data analysis for sparse longitudinal data. *Journal of the American Statistical Association*, 100:577–590.
- Zhang, S., Jank, W., and Shmueli, G. (2010). Real-time forecasting of online auctions via functional k-nearest neighbors. *International Journal of Forecasting*, 26:666–683.